

## ON THE DISTRIBUTION AND SCALING OF CONVECTIVE WAVESPEEDS IN THE SHEAR LAYERS OF HEATED, SUPERSONIC JETS

**Tobias Ecker**

Dept. of Aerospace and Ocean Engineering  
 Virginia Tech  
 215 Randolph Hall, Blacksburg (VA), USA  
 ecker@vt.edu

**K. Todd Lowe**

Dept. of Aerospace and Ocean Engineering  
 Virginia Tech  
 215 Randolph Hall, Blacksburg (VA), USA  
 kelowe@vt.edu

**Wing F. Ng**

Dept. of Mechanical Engineering  
 Virginia Tech  
 440 Goodwin Hall, Blacksburg (VA), USA  
 ng@vt.edu

### ABSTRACT

The noise generated by supersonic plumes is of growing concern given the enormous peak noise intensity radiated by tactical aircraft engines. A key component of this noise is the enhanced radiation of mixing caused by supersonic eddy speeds. As very little data exist for eddy convection in high Reynolds number, supersonic plumes, our current ability to develop concepts that alter compressible eddy convective is limited. Herein we present new experimental data and a phenomenological description of eddy wave-speeds in the developing shear layer of supersonic heated jets. A new scaling of the wavespeed in radial similarity coordinates is proposed which takes into account the influence of the ratio of static densities between the jet and ambient streams. The frequency-dependent behavior of the convective velocity reflects the process of high momentum, high velocity large-scale eddies pinching off from the potential core and convecting into regions of locally reduced mean velocities. In particular, we observe a structural change in wavespeed spectra at the end of the potential core. In addition to high turbulence levels, the potential core breakdown region can have enhanced eddy speeds, increasing noise radiation efficiency.

### INTRODUCTION

Recent theoretical and computational work (Papamoschou et al., 2014) has built upon earlier concepts (Papamoschou, 1997) for peak noise reduction by altering the convective Mach number of eddies in the shear layer of jet plumes. Papamoschou points out via acoustic analogy that noise in high speed plumes has two components — a scaling of the source provided by turbulent fluctuation amplitudes and a radiation efficiency contribution shown to be a function of the acoustic eddy convective Mach number,  $M_a = U_c/a$ , where the speed of sound  $a$  is that of the surrounding ambient medium. While reducing the large-scale eddy turbulence in plumes is possible, considerable effort on the topic has, to date, yielded limited success. Further, the noise produced scales linearly with turbulence intensity. As such, a 50% reduction in turbulence intensity, equates to a 3 dB noise

reduction—a modest noise impact for such a miraculous turbulence reduction. In contrast, the radiation efficiency — the amount of turbulent kinetic energy that will be converted to acoustic energy — scales nonlinearly with eddy convective Mach number and offers considerably more latitude for noise reduction.

The convection of turbulent fluctuations in shear flows is directly related to the process of noise generation and propagation. Several theories based on acoustic analogies derived by Lighthill (1952) directly relate the pressure fluctuations and the noise intensity to fourth order correlations and the eddy convective velocity. Bailly et al. (1997) summarize the relevant aspects with regards to the convective amplification factor for models by Ribner, Goldstein-Howes and Ffowcs Williams and Maidanik. In all models the convective Mach number, based on the eddy convective velocity can be identified as a driver of the produced noise intensity and similarly the radiation efficiency (Papamoschou et al., 2014).

The relative convective Mach number is defined as the ratio of the convective velocity to the sound speed,

$$M_c = (U_j - u_c)/a_j \quad (1)$$

where  $U_j$  and  $a_j$  are the isentropic exit velocity and sound speed, respectively. For co-annular jet flows or shear layers, high speed stream often carries the subscript (1), whereas the lower speed stream is notated as (2). The theoretical (symmetric) convective Mach number is defined (Papamoschou 1997):

$$M_{c\ sym} \equiv (U_1 - U_2)/(a_1 + a_2) \quad (2)$$

For a single-stream jet at perfectly expanded condition and same gas properties as the ambient gas, a relationship between the isentropic jet Mach number  $M_j$  and the symmetric convective Mach number  $M_{c\ sym}$  can be easily derived,

$$M_{c\ sym} = M_j / (1 + \sqrt{\rho_a/\rho_j}) \quad (3)$$

revealing a simple dependence on the ratio of ambient density to core density,  $\rho_a/\rho_j$ .

Convective velocity may be considered at the integral scale or as a function of frequency/wave-number (Wills,

1964). The frequency-dependent convective velocity, due to the existence of differently sized eddies moving at different convective velocities within the turbulent field, indicates a detachment between the turbulent frequency and wave-number spectra and divergence from Taylor's frozen turbulence hypothesis.

Fisher and Davies (1964) studied the validity of Taylor's hypothesis in shear flows via two-point cross-correlation using hot wire anemometry and found a clear frequency dependence of the convective velocity from their experimental results. Davis et al. (1964) studied the subsonic round jet and found flares of strong fluctuations of  $(-u')$  adjacent to the core (region I in figure 1) and  $(+u')$  in the outer region (region II in figure 1). These observations are consistent with subsequent studies that provide the established distribution of mean and integral convective velocities within a jet shear layer (figure 1). Large eddies strongly influence this observed structure.

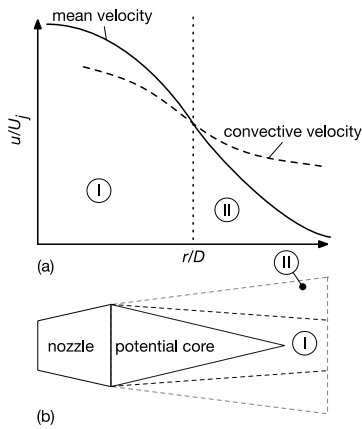


Figure 1. (a) Mean and convective velocity distribution over the jet radius. (b) Indication of the two different convective velocity regions through the jet domain.

Previous studies (de Kat et al., 2013) have shown limitations in determining wave-number dependent convective velocities due to the effect of low pass filtering of PIV on the power spectra. Restrictions due to the characteristics of the phase spectrum are analyzed and general limiting conditions for experimental parameters not only limited to PIV are summarized. Kerhervé et al. (2004b) demonstrated the frequency dependency of the turbulence scales in sub- and supersonic jet flows from their non-evenly sampled laser Doppler velocimeter (LDV) data. The study indicated that limitations due to noise and data-rate appear to influence the spectra and the derived phase angles.

The frequency-dependent wave-speed may be found from the phase difference between the signals at stations  $i$  and  $j$ ,

$$u_c(f) = 2\pi f \Delta x / \phi_{ij}(f) \quad (4)$$

where the phase is found from the cross-spectrum,  $G_{ij}$ ,

$$\phi_{ij}(f) = \tan^{-1}(\text{Im}[G_{ij}] / \text{Real}[G_{ij}]) \quad (5)$$

Due to spatial aliasing, the estimated limiting maximum Strouhal number for wave-speed measurement is

$$Sr_{high} < (u_c / U_j)(D / 2\Delta x) \quad (6)$$

where  $D$  is the nozzle diameter. Alternatively to the spectral approach, a narrow band-pass filter approach can be used to generate narrowband time signals for time delay cross-correlation processing (e.g., Fisher and Davies 1964).

In the present work, a very high repetition rate, multi-point velocimetry instrument based upon the time-resolved Doppler global velocimetry (TR-DGV) technique (Ecker et al. 2014a; 2014b) is used to obtain convective wave-speed measurements in heated, supersonic jets. The processing methods developed are discussed to follow.

## DATA PROCESSING

In order to determine the sensitivity of wave-speed estimates to different data processing parameters, studies using Monte-Carlo simulations were performed.

The model signals are constructed from a one-dimensional model turbulent power spectrum (Pope 2000) with each signal given a random phase spectrum. The mean velocity and the turbulence intensity of the dataset used were set at 650 m/s and 10%, respectively. The phase of this dataset is then evolved based on the separation between four flow sensors using an empirical fit given by Morris and Zaman (2010), thus creating a non-linear phase angle in the cross-spectrum between stations. The separation distances were the same as the actual physical sensor spacing used in this study.

Two processing techniques were considered: (1) reconstruction based on the phase angle, (2) digital band-pass filtering in combination with time delay cross-correlation processing. Figure 2 shows the reconstructed convective velocity profile using both the phase method and the band-pass filter method for two signal to noise ratios.

The processing parameters investigated are: (1) ratio of averaged sets length  $S$  to dataset length  $N$  and (2) ratio of window length  $W$  (at 50% overlap) to subset length  $S$  at a fixed dataset length ( $N = 100k$  samples). Further (3) the signal to noise ratio ( $SNR_{log}$ ), (4) the type of window (Square, Hanning, Hamming) and the (5) magnitude of the convective wave speed  $u_c$ . Table 1 presents all the cases considered in this sensitivity analysis.

The results indicate that a small subset length and a small window size lead to lowest RMS errors. Only a minimal sensitivity to the mean convective velocity, which imposes a time shift between the signals at the two stations, has been noted. Errors tend to be slightly higher for higher convective velocities as the phase angles are shallower and therefore more sensitive to noise. Convective velocities at very low frequencies were found to be inherently uncertain and frequencies below  $f_{low} = 0.1(U_j / 2\Delta x)$  were excluded from the statistics.

The narrowband filter method was implemented by applying a narrow band-pass filter to the data set before performing time delay cross-correlation processing. The digital band-pass filter used is based on a fast Fourier transform (FFT) method. The cases considered in the analysis of the performance of the filter are summarized in table 2.

The dependence of the RMS error on  $SNR_{log}$  and window type is shown in figure 3. The phase method requires very high  $SNR_{log}$  to be effective, whereas the filter method is very robust even down to  $SNR_{log} = 5$  dB. Above 12.5 dB the error due to the processing is about  $\pm 1\%$  of the  $u_c/U_j$  for the filter technique. Due to the robustness at low  $SNR_{log}$  the filter method is used to obtain all results presented within this study.

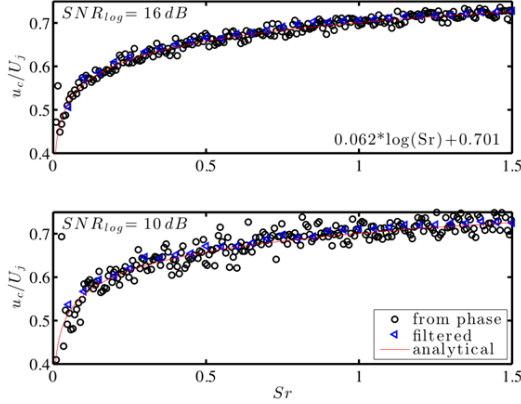


Figure 2. Reconstructed convective velocity versus Strouhal number for both phase method and band-pass filtered method.

Table 1. Monte Carlo parameters for the phase method.

Case	Window	$S/N$	$W/S$	$SNR_{log}$	$u_c/U_j$
HN1	Hanning	0.2	0.2	-5 - 20	profile
SQ1	Square	0.2	0.2	-5 - 20	profile
HM1	Hamming	0.2	0.2	-5 - 20	profile
HN2	Hanning	0.2-1	0.2-1	20	profile
HN3	Hanning	0.2	0.2	20	0.3-0.9

Table 2. Monte Carlo parameters for the filter method.

Case	Window	$S/N$	$SNR_{log}$	$u_c/U$
FHN	Hanning	0.2	-5 - 20	profile
FSQ	Square	0.2	-5 - 20	profile

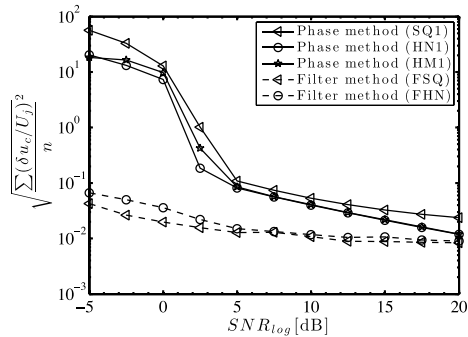


Figure 3. RMS error of the convective velocity dependent on the signal to noise ratio and the window type used (cases HN1, SQ1, HM1, FSQ, FHN).

## EXPERIMENTAL APPARATUS AND FACILITY

The laser-based time-resolved DGV (TR-DGV) concept used in this study has frequency response to 125 kHz and three-velocity-component capability at 32 simultaneous points in the flow and a contiguous acquisition time of greater than one second. The TR-DGV instrument and the PMT sensor system used, are documented by Ecker et al. (2014b, 2015). It offers advantages in the current study over high spatial resolution approaches since sample sets were very large in time and correlations were measurements over very short distances and times, over which eddy speeds would be constant.

The Virginia Tech hot jet facility has been described in past works (Ecker et al., 2014a). This electrically heated (192 kW) free jet facility provides supersonic flow at total temperature ratios  $T_0/T_a$  up to 3 at 0.12 kg/s mass flow rate. The bi-conic nozzle used ( $M_d = 1.65$ ) is an axisymmetric adaptation of the geometry studied by Powers and McLaughlin (2012) for military-style nozzles. The diameter  $D$  of the nozzle exit is 38.1 mm. Flow seeding is 0.2-0.3  $\mu\text{m}$  alumina dispersed by a cyclone seeder unit. Co-flow seeding was provided by a ViCount smoke generator producing mineral oil droplets of approximately 0.3  $\mu\text{m}$  diameter.

## Test matrix and geometry

For this study two cases (identified as A and B) at two different total temperature ratio (TTR) conditions at four different streamwise locations ( $x/D = 4, 6, 8$  and 10) were experimentally investigated. The parameters of the two cases are presented in table 3. Recording time length was 1 s with an effective data rate of 250 kHz.

A drawing of the bi-conic nozzle and the flow plane sensor configuration are displayed in figure 4. The streamwise coordinate  $x/D$  on the centerline is defined as the distance from the nozzle exit plane to the center of the flow plane sensor (red). The radial coordinate  $r/D$  is defined as the distance from the centerline to the each sensor pixel. The distance between pixels is 3 mm.

Table 3. Hot jet cases.

Case	$Re$	$M_j$	$\rho_j/\rho_a$	TTR
A	1.3M	1.68	0.96	1.63
B	1.15M	1.70	0.79	2.0

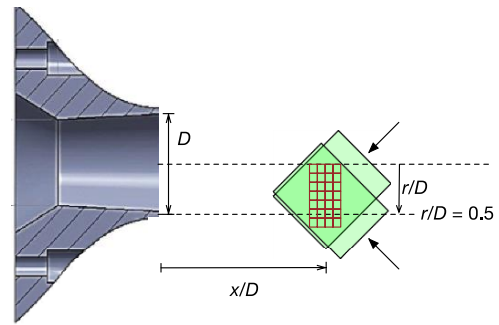


Figure 4. Nozzle and sensor configuration and nomenclature.

## RESULTS

The mean velocity and turbulence statistics have previously been investigated by Brooks and Lowe (2014). As shown in previous studies (Lau, 1980), the mean velocity as well as normal and shear stresses can be collapsed radially with a similarity scaling based on the radial location of 50% of the jet exit velocity and linear shear layer growth.

$$\eta^* = (r - r_{0.5U_j})/x \quad (10)$$

where  $r_{0.5U_j}$  is the radius at which the flow is  $\frac{1}{2}$  the jet core velocity. The results for the mean velocity distribution of this jet, compared with results from studies by Kerhervé et al. (2004a) and Lau et al. (1979), are shown in figure 5.

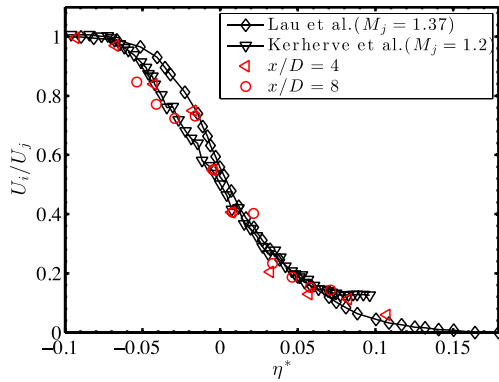


Figure 5. Similarity profiles for the streamwise mean velocity for case B at  $x/D = 4$  and 8 compared to other studies.

### Integral convective velocity

Few studies of the radial distribution of the integral convective velocity in round, incompressible *or* compressible jets exist. Applying the same similarity scaling which successfully collapses the mean velocity has only led to partial collapse for the case of the convective velocity.

To better understand the drivers for the structure of convective velocity profiles, we propose a similarity scaling based on the symmetric convective Mach number and the density ratio,

$$\eta_c = K^2(r - r_{0.5M_{c\,sym}})/x \quad (11)$$

where

$$K = \left( \rho_j/\rho_a + M_{c\,sym}^2(\gamma - 1)/2 \left[ 1 + \sqrt{\rho_j/\rho_a} \right]^2 \right) \quad (12)$$

It is to note that this scaling is solely based on flow parameters and contains no empirical constants.

Figure 6 shows the collapse for convective velocity data from various Mach numbers and density ratios at different streamwise locations for the current study as well as several cases from the literature (table 4).

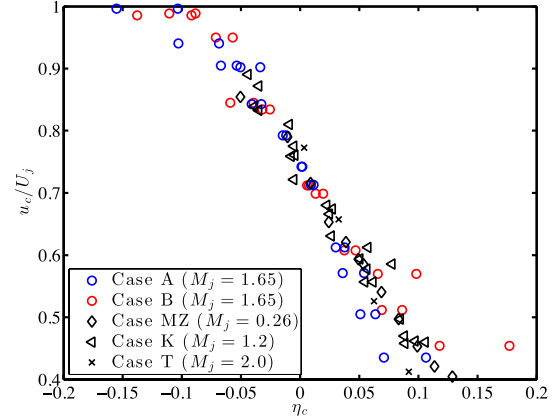


Figure 6. Similarity profiles for the streamwise integral convective velocity for case A and B (see table 3), as well as different literature cases (see table 4).

Table 4. Literature cases.

Case	Reference	$Re$	$M_j$	$\rho_j/\rho_a$	$TTR$
MZ	Morris and Zaman 2010	0.24M	0.26	0.98	1.0
K	Kerhervé et al. 2004b	1.1M	1.2	0.77	1.0
T	Thurow 2005	2.6M	2.0	0.55	1.0

### Convective velocity frequency dependence

The frequency dependent convective velocities in the shear layer ( $r/D = 0.28$ ) at position before ( $x/D = 8$ ) and close to the mean flow potential core length ( $x/D = 10$ ) are shown in figure 7. At  $x/D = 8$  (figure 7, top) a distribution similar to previously reported data (e.g. Morris and Zaman, (2010, Kuo et al., 2011 and Goldschmidt et al. 1981) is observed. This distribution shows an rapid increase of convective velocity up to  $Sr = 0.5$ , followed by a more gradual increase after. For the investigated frequencies, which are limited by temporal and spatial aliasing, no convergence to the local mean velocity value is observed. The distribution of the convective velocities further downstream presents very differently (figure 7, bottom); at low  $Sr$  the convective velocity rises rapidly and reaches a distinctive peak close to the integral convective velocity value near  $Sr = 0.45$ . Above this value the convective velocity decreases to a plateau.

The convective velocity data near the centerline ( $r/D = 0$ ) are shown in figure 8. The convective velocity distribution shows similar features as before but is less pronounced due to the upstream vicinity of the potential core, which is not broken down completely.

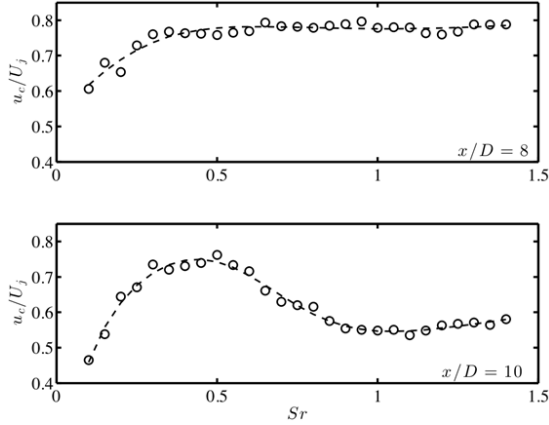


Figure 7. Convective velocity scaling with frequency at  $r/D = 0.28$  at  $x/D = 8$  (top) and  $x/D = 10$  (bottom) for case B; circles are measured data, dashed line for visualization purposes.

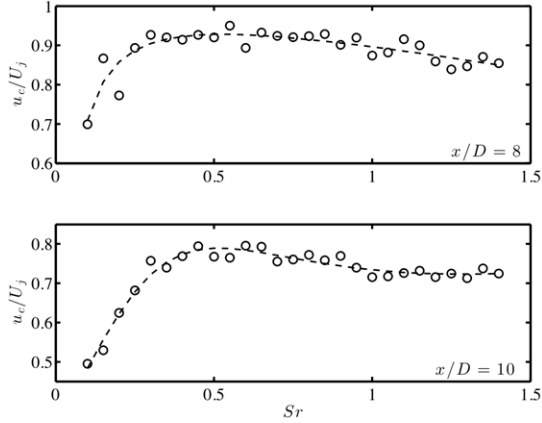


Figure 8. Convective velocity scaling with frequency at  $r/D = 0.039$  at  $x/D = 8$  (top) and  $x/D = 10$  (bottom) for case B; circles are measured data, dashed line for visualization purposes.

These frequency-dependent results lay the basis to conceptually explain a key component of the high noise emissions present in heated supersonic jets. Large scale turbulent eddies, energized from the mean flow potential core, intermittently convect into regions of lower local mean velocity. These events create eddies with high local convective Mach numbers such that their disturbances couple more efficiently to the far field, e.g., according to the analogy of Papamoschou et al. (2014).

This conceptual relationship between the potential core breakdown and eddy convection speeds is displayed in figure 9. Highly energized eddies moving from region (I) into region (II) transport high momentum remnants of irrotational fluid from the potential core and create a zone with highest convective amplification values. This zone is located downstream of, and also surrounding, the mean potential core. These irrotational fluid packets are then exposed to the shear layer mean velocity gradient, leading to the formation of ring vortex-like eddies.

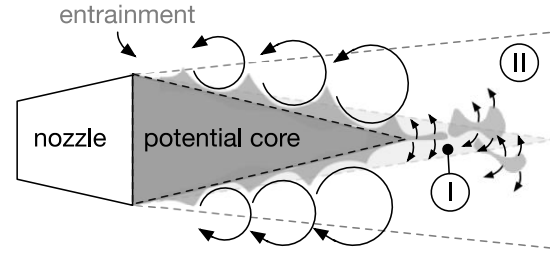


Figure 9. Conceptual relationship between the mean and convective velocity creating regions of high radiation efficiency.

The region just beyond the potential core has previously been identified as a strong sound-producing zone by Hileman and Samimy (2006). Similarly Mora et al. (2014) found significant growth of pressure fluctuation skewness values in the shear layer surrounding the potential core region. Results from a direct numerical simulation of a slightly heated supersonic jet ( $M_j = 1.92$ ), coupled with a linear wave equation model for the far field indicate increased pressure fluctuations consistent with Mach wave radiation emanating from the end of the potential core (Freund et al., 2000). A qualitative interpretation of the dilatation contours indicates an increase in noise emission towards the location of the mean velocity potential core breakdown. Presented overall sound pressure levels corroborate this observation.

The present study indicates that the increased diffusion of the mean velocity field due to the heating leads to a pronounced effect of distribution of eddy convective velocity—and thus on noise radiation. As is well understood, the effects of heating are not limited to increased fluid speed relative to the ambient sound speed. It seems likely that the structural changes in the flow result in fundamental re-scaling of the convective phenomena that produce peak noise intensity. The conceptual model presented provides a framework for future analyses to obtain representative inputs to noise radiation terms that depend upon convective wave-speed.

It is also evident from the presented experimental convective velocity distributions and the observations made in past studies, that intermittency effects must play a key role and are strongly coupled with the process of fast convecting eddies entering slower regions of the flow.

## CONCLUSIONS

A heated supersonic jet at two different density ratios was experimentally investigated for the scaling of the eddy convective velocities. Radial profiles of the convective velocity were presented and successfully collapsed with previous data at different conditions by accounting for density ratio and symmetric convective Mach number. The difference in diffusion of the mean velocity field and the integral eddy convective velocity indicates regions of locally high convective Mach numbers and increased radiation efficiency. The investigation of the scaling of the convective velocity with

frequency at several locations in the shear layer and near the centerline demonstrated the intrusion of high momentum, large-scale eddies. The region just downstream of the potential core is identified as the main zone of this phenomenon. It is hypothesized that this large-scale, intermittent effect is one of the key drivers of peak noise emissions in heated supersonic jets.

The authors acknowledge the support of the Office of Naval Research under grants N00014-11-1-0754 and N00014-12-1-0803, program managers Brenda Henderson and Joseph Doychak.

## REFERENCES

- Bailly, C., Lafon, P., Sé, and Candel, B., 1997, "Subsonic and supersonic jet noise predictions from statistical source models", *AIAA Journal*, Vol. 35, No.11, pp. 1688-1696.
- Brooks, D. R., & Lowe, K. T., 2014, "Fluctuating Flow Acceleration in a Heated Supersonic Jet", *Presented at the 12th International Symposium on Applications of Laser Techniques to Fluid Mechanics*, Lisbon.
- de Kat, R., Gan, L., Dawson, J. R., and Ganapathisubramani, B., 2013, "Limitations of estimating turbulent convection velocities from PIV", *arXiv.org*.
- Ecker, T., Brooks, D. R., Lowe, K. T., and Ng, W. F., 2014a, "Development and application of a point Doppler velocimeter featuring two-beam multiplexing for time-resolved measurements of high-speed flow", *Experiments in Fluids*, Vol. 55 No. 9, pp. 1–15.
- Ecker, T., Lowe, K. T., and Ng, W. F., 2015, "A rapid response 64-channel photomultiplier tube camera for high-speed flow velocimetry", *Measurement Science and Technology*, Vol. 26, No. 2, 027001.
- Ecker, T., Lowe, K. T., Ng, W. F., and Brooks, D. R., 2014b, "Fourth-order Spectral Statistics in the Developing Shear Layers of Hot Supersonic Jets", *Presented at the AIAA Propulsion and Power (50th AIAA/ASME/SAE/ASEE Joint Propulsion Conference)*, Cleveland, OH.
- Fisher, M. J., and Davies, P. O. A. L., 1964, "Correlation measurements in a non-frozen pattern of turbulence", *Journal of Fluid Mechanics*, Vol. 18, pp. 97–116.
- Freund, J. B., Lele, S. K., and Moin, P., 2000, "Numerical Simulation of a Mach 1.92 Turbulent Jet and Its Sound Field", *AIAA Journal*, Vol. 38, No. 11, pp. 2023-2031.
- Goldschmidt, V. W., Young, M. F., and Ott, E. S., 1981, "Turbulent convective velocities (broadband and wavenumber dependent) in a plane jet", *Journal of Fluid Mechanics*, Vol. 105, pp. 327–345.
- Hileman, J. I., and Samimy, M., 2006, "Mach Number Effects on Jet Noise Sources and Radiation to Shallow Angles", *AIAA Journal*, Vol. 44, No. 8, pp. 1915–1918.
- Mora, P., Heeb, N., Kastner, J., Gutmark, E. J., and Kailasanath, K., 2014, "Impact of Heat on the Pressure Skewness and Kurtosis in Supersonic Jets", *AIAA Journal*, Vol. 52, No. 4, pp. 777–787.
- Morris, P. J., and Zaman, K. B. M. Q., 2010, "Velocity measurements in jets with application to noise source modeling", *Journal of Sound and Vibration*, Vol. 329, No. 4, pp. 394–414.
- Kerhervé, F., Jordan, P., Gervais, Y., and Valiere, J. C., 2004a, "Two-point laser Doppler velocimetry measurements in a Mach 1.2 cold supersonic jet for statistical aeroacoustic source model", *Experiments in Fluids*, Vol. 37, No. 3, pp. 419–437.
- Kerhervé, F., Power, O., Fitzpatrick, J., and Jordan, P., 2004b, "Determination of Turbulent Scales in Subsonic and Supersonic Jets from LDV Measurements", *Presented at the 12th International Symposium on Applications of Laser Techniques to Fluid Mechanics*, Lisbon.
- Kuo, C. W., Powers, R., and McLaughlin, D. K., 2011, "Space-time correlation of flow and acoustic field measurements in supersonic helium-air mixture jets using optical deflectometry", *17th AIAA/CEAS Aeroacoustics Conference (32nd AIAA Aeroacoustics Conference)*, Portland, Oregon.
- Lau, J. C., 1980, "Laser velocimeter correlation measurements in subsonic and supersonic jets", *Journal of Sound and Vibration*, Vol. 70, No. 1, pp. 85–101.
- Lau, J. C., Morris, P. J., and Fisher, M. J., 1979, "Measurements in subsonic and supersonic free jets using a laser velocimeter", *Journal of Fluid Mechanics*, Vol. 93, pp. 1–27.
- Lighthill, M. J., 1952, "On Sound Generated Aerodynamically. I. General Theory", *Proceedings of the Royal Society A: Mathematical, Physical and Engineering Sciences*, Vol. 211, No. 1107, pp. 564–587.
- Papamoschou, D., 1997, "Mach wave elimination in supersonic jets", *AIAA Journal*, Vol. 35, No. 10, pp. 1604-1611.
- Papamoschou, D., Xiong, J., and Liu, F., 2014, "Reduction of Radiation Efficiency in High-Speed Jets", *Presented at the AIAA Aviation, 20th AIAA/CEAS Aeroacoustics Conference*, Atlanta, GA.
- Pope, S. B., 2000, *Turbulent Flows*, Cambridge University Press.
- Powers, R. W., and McLaughlin, D. K., 2012, "Acoustic measurements of scale models of military style supersonic beveled nozzle jets with interior corrugations", *Presented at the 18th AIAA/CEAS Aeroacoustics Conference (33rd AIAA Aeroacoustics Conference)*, Colorado Springs, CO.
- Thurrow, B. S., 2005, *On the convective velocity of large-scale structures in compressible axisymmetric jets*, PhD Thesis, The Ohio State University, Columbus, OH.
- Wills, J. A. B., 1964, "On convection velocities in turbulent shear flows", *Journal of Fluid Mechanics*, Vol. 20, No. 3, pp. 417–432.